

## An edge detection approach based on directional wavelet transform<sup>☆</sup>

Zhen Zhang<sup>a,b,\*</sup>, Siliang Ma<sup>a</sup>, Hui Liu<sup>a</sup>, Yuexin Gong<sup>a</sup>

<sup>a</sup> Institute of Mathematics, Jilin University, Changchun 130012, PR China

<sup>b</sup> Daqing Petroleum, CNPC, Daqing 163453, PR China

### ARTICLE INFO

#### Article history:

Received 11 July 2007

Received in revised form 17 March 2008

Accepted 8 November 2008

#### Keywords:

Edge detection

Directional wavelet transform

Feature extraction

Non-maximum suppression

Image processing

### ABSTRACT

The standard 2D wavelet transform (WT) has been an effective tool in image processing. In recent years, many new transforms have been proposed successively, such as curvelets, bandlets, directional wavelet transform etc, which inherit the merits of the standard WT, and are more adequate at the 2D image processing tasks. Intuitively, it seemed that applying these novel tools to edge detection should acquire finer performance. In this paper, we propose an edge detection approach based on directional wavelet transform which retains the separable filtering and the simplicity of computations and filter design from the standard 2D WT. In addition, the corresponding gradient magnitude is redefined and a new algorithm for non-maximum suppression is described. The experimental results of edge detection for several test images are provided to demonstrate our approach.

© 2009 Elsevier Ltd. All rights reserved.

### 1. Introduction

The edge detection is very useful in image processing and computer vision, as it can locate significant variations of gray images [1,2]. The edges are often interpreted as one class of singularities in an image. For a continuous function, singularities can be characterized easily as discontinuities where the gradient approaches infinity. However, image data is discrete, so edges in an image are often defined as the local maxima of the gradient. The gradient-based edge detectors are basically a high-pass filter which can be applied to enhance the edge points in an image, such as Roberts, Sobel and Prewitt operators [3–5]. The classical edge detectors usually work well with high-quality images, but are not good enough for noisy images because of using a small kernel to convolve an image. In order to overcome these problems, Canny described an edge detection approach based on gradient, whose filter can be closely approximated by the first-order derivative of the Gaussian function. Up until now, it has already become one of the most popular edge detector [6]. The approach based on standard WT presented by Mallat and his colleagues is also a representative gradient approach [7,8], and Canny edge detection is equivalent to finding the local maxima of the wavelet transform.

The standard 2D WT has a long and successful history as an efficient image processing tool. Its application is most frequently based on a separable transform, that is, rows and columns in an image are treated independently. Such a method keeps simplicity in design and computation. However, as a result of the separable transform given by the tensor-product of two 1D wavelets along the horizontal and vertical directions, the standard 2D WT can only capture very limited directional information. This separable transform is good at isolating horizontal and vertical edges, but it is not adequate for treating more complex discontinuities.

Recently, a number of approaches that can provide finer direction analysis are proposed. The ridgelet and the curvelet transforms were proposed by Candés and Donoho [9,10]. Both transforms show the potential of non-separable methods,

<sup>☆</sup> This research was supported by the China National Petroleum Corporation.

\* Corresponding author at: Institute of Mathematics, Jilin University, Changchun 130012, PR China.

E-mail address: [zhangzhq99@163.com](mailto:zhangzhq99@163.com) (Z. Zhang).

but come at a price in terms of design and computation complexity. Indeed, ridgelet and curvelet are defined in continuous spaces and the construction of equivalent transforms in discrete spaces is not trivial. Other non-separable approaches, such as directional filter banks [11,12] and steerable pyramid [13], suffer from similar drawbacks. Some separable approaches have been made in [14] but not on discrete spaces. Finally, the bandlet proposed by Mallat and LePennec [15] and the edge adapted multiscale transform of Cohen and Matei [16] require an edge detection step followed by an adaptive transform, for this reason these methods tend to be complex.

In our approach, we wish to retain the simplicity of separable wavelet transforms, while realizing some potential of the non-separable schemes. We do this by adopting the directional wavelet transform that acts much like a standard separable transform, but allowing more directions [17,18]. This separable discrete directional wavelet transform is implemented based on lattice theory. In addition, in order to sufficiently make use of more directional information provided by directional wavelet transforms, we redefine gradient magnitude and describe a new algorithm for non-maximum suppression.

## 2. Directional wavelet transforms based on lattice theory

### 2.1. Lattice-based sampling

In order to apply a discrete transform in the discrete space  $\mathbb{Z}^2$  along a certain direction, we need to sample the pixels that are located at the chosen direction. Now we describe a novel method applying sampling along the certain directions. First, we give the definition of continuous line.

**Definition 2.1.** The continuous line  $l(r, b)$ , where  $r, b \in \mathbb{R}$ , is defined as the set of points  $(x, y) \in \mathbb{R}^2$  such that:

$$y = rx + b. \quad (1)$$

A continuous line  $l(1/2, b)$  is shown (the thin line) in Fig. 1(a).

The discrete approximation of (1) is called digital line  $L(r, k)$ . Next, we give the definition of the digital line.

**Definition 2.2.** Given a rational slope  $r$ , the digital line  $L(r, k)$ , where  $k \in \mathbb{Z}$ , is defined as the set of pixels  $(i, j)$  such that:

$$\begin{aligned} j &= \lceil ri \rceil + k, \quad \forall i \in \mathbb{Z}, \text{ for } |r| \leq 1, \quad \text{or} \\ i &= \lfloor j/r \rfloor + k, \quad \forall j \in \mathbb{Z}, \text{ for } |r| > 1. \end{aligned} \quad (2)$$

A digital line  $L(1/2, k)$  is shown (the bold line) in Fig. 1(a).

Finally, we introduce the concept of sampling-line. A given vector  $[m, n]$ , where both  $m$  and  $n$  are integers, can determine a rational transform direction. Let full-rank integer lattice  $\Lambda$  consist of the points obtained as linear combinations of the vectors  $[m, 0]$  and  $[0, n]$ , it is a sublattice of the cubic integer lattice  $\mathbb{Z}^2$ , that is,  $\Lambda \subset \mathbb{Z}^2$ . The lattice  $\Lambda$  can be represented by a non-unique generator matrix

$$M_\Lambda = \begin{pmatrix} m & 0 \\ 0 & n \end{pmatrix} = \begin{pmatrix} \mathbf{p} \\ \mathbf{q} \end{pmatrix} \quad \text{where } m, n \in \mathbb{Z}. \quad (3)$$

Recall that the cubic lattice  $\mathbb{Z}^2$  can be partitioned into  $|\det(M_\Lambda)|$  cosets of the lattice  $\Lambda$  [19], where each coset is determined by the shift vector  $d_f, f = 0, 1, \dots, |\det(M_\Lambda)| - 1$ . Therefore, the lattice  $\Lambda$  with the corresponding generator matrix  $M_\Lambda$  given by (3) partitions each digital line  $L(r = n/m, k)$  into sampling-lines.

**Definition 2.3.** The sampling-line  $SL_{d_f}(r, k)$ , where  $r = n/m$ , and  $m, n, k \in \mathbb{Z}$ , is defined as the intersections between the digital line  $L(r, k)$  and the  $f$ th coset of the lattice  $\Lambda$ .

Sampling-lines  $SL_{[0,0]}(1/2, k)$  and  $SL_{[1,0]}(1/2, k)$  are shown in Fig. 1(b). Notice that a sampling-line is simply the intersections between a coset and digital line.

### 2.2. Directional wavelet transforms along sampling-lines

Consider a special class of wavelets which can be defined as the derivative of the smoothing function, and the Gaussian is chosen as the smoothing function, that is,

$$\theta(t) = \frac{1}{\sqrt{2\pi}} \exp(-t^2/2), \quad (4)$$

$$\text{then, } \psi(t) = \frac{d\theta}{dt} = \frac{-t}{\sqrt{2\pi}} \exp(-t^2/2). \quad (5)$$

$$\text{Notice : } \int_{-\infty}^{+\infty} \frac{-t}{\sqrt{2\pi}} \exp(-t^2/2) dt = 0. \quad (6)$$

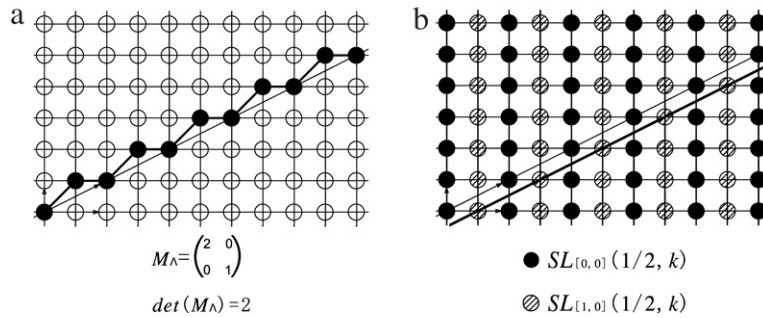


**Fig. 1.** (a) A continuous line  $y = 1/2x + b$  and a digital line  $L(1/2, k)$ ; (b) Intersections between the two cosets of the lattice  $\Lambda$  given by the generator matrix  $M_A$  and the digital lines  $L(1/2, k)$ , where  $k \in \mathbb{N}$ , are the sampling-lines  $SL_{[0,0]}(1/2, k)$  and  $SL_{[1,0]}(1/2, k)$ .

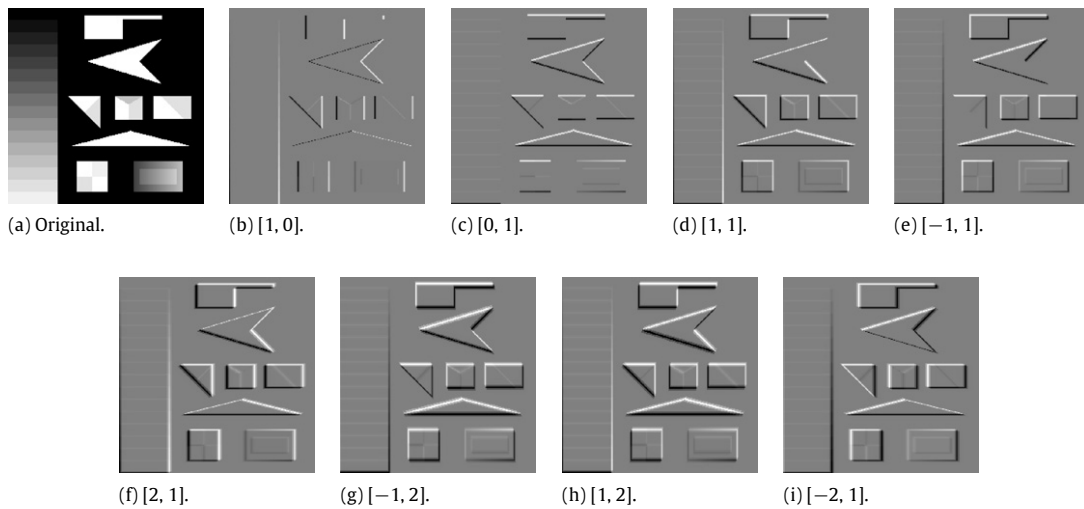


**Fig. 2.** (a) Original image; (b)–(i) The results of directional wavelet transforms along the directions  $[1, 0]$ ,  $[0, 1]$ ,  $[1, 1]$ ,  $[-1, 1]$ ,  $[2, 1]$ ,  $[-1, 2]$ ,  $[1, 2]$ ,  $[-2, 1]$  respectively.

**Definition 2.4.** The continuous wavelet transform of a function  $f(t) \in L^2$  with respect to an analyzing wavelet  $\psi$  is defined as:

$$WT_f(a, b) = \int_{-\infty}^{+\infty} f(t)\psi_{a,b}(t)dt, \tag{7}$$

where  $\psi_{a,b}(t) = \frac{1}{\sqrt{a}}\psi\left(\frac{t-b}{a}\right)$ ,  $a > 0$ , and  $\psi(t)$  satisfies the following condition:

$$\int_{-\infty}^{+\infty} \psi(t)dt = 0. \tag{8}$$

Wavelet transforms can be computed by convolving the signal with a wavelet, so the wavelet transform of  $f(t)$  at the scale  $a$  and position  $b$  is denoted as:

$$WT_f(a, b) = \sqrt{a}f * \bar{\psi}_a(b), \tag{9}$$

$$\text{where } \bar{\psi}_a(t) = a^{-1}\psi(-t/a). \tag{10}$$

$\bar{\psi}_a(t)$  can be considered as a high-pass filter.

Now, we apply directional wavelet transforms. The eight transform directions,  $\{[1, 0], [0, 1], [1, 1], [-1, 1], [2, 1], [-1, 2], [1, 2], [-2, 1]\}$ , are chosen, and the results of the transforms are shown in Fig. 2.

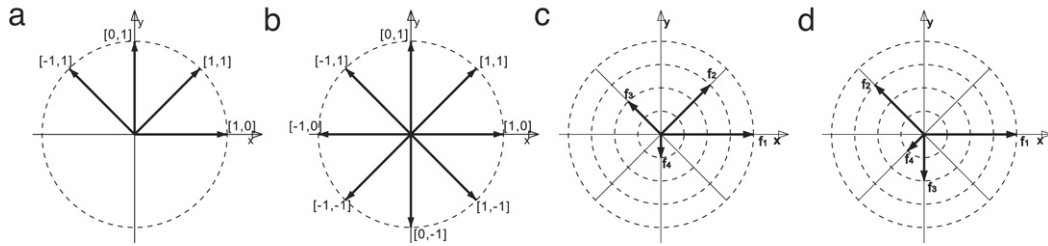


**Fig. 3.** (a) Four directions of directional wavelet transform; (b) Eight directions of directional derivative might be generated by directional wavelet transforms; (c) (d) Two cases of transform results.

### 3. Edge detection and location

#### 3.1. General steps of edge detection algorithm based on gradient

##### Step 1: Pre-smooth the image

In order to reduce the influence of noise, an image is first smoothed by a smoothing filter.

##### Step 2: Enhance edges of the image

Convolve the image  $f(x, y)$  with a gradient operator along the horizontal and vertical directions, and then the gradient magnitude and orientation, which are defined by  $\|\nabla f\|_2 = \sqrt{f_x^2 + f_y^2}$  and  $\theta = \arctan(f_y/f_x)$ , are computed respectively.

##### Step 3: Non-maximum suppression

For each pixel, check whether it is a local maximum along the gradient direction, and retain it if is.

##### Step 4: Locate and link edges adopting double threshold scheme

A high  $\tau_1$  threshold is selected such that all pixels with gradient magnitude greater than  $\tau_1$  are classified as edge elements. A low threshold  $\tau_2 < \tau_1$  is selected such that all pixels with gradient magnitude greater than  $\tau_2$  and smaller than  $\tau_1$  are classified as candidate edges. If a candidate edge in the direction perpendicular to the gradient is a neighborhood of an edge, then the candidate is reclassified as an edge too.

How to sufficiently make use of more directional information provided by directional wavelet transforms is vital for edge detection and location. Meanwhile, consider the discrete property of image data, it is unsuitable that the gradient magnitude and direction are simply defined as  $\|\nabla f\|_2 = \sqrt{f_x^2 + f_y^2}$  and  $\theta = \arctan(f_y/f_x)$ . In our approach, the gradient magnitude is redefined and a new algorithm for non-maximum suppression is described.

#### 3.2. Redefinition of gradient magnitude

Although the transforms can be applied along any directions, only four transform directions  $\{[1, 0], [0, 1], [1, 1], [-1, 1]\}$  are chosen because of considering computational complexity and correlation among pixels. The corresponding gradient magnitude is defined as follows:

**Definition 3.1.** The gradient magnitude of a point  $f(x, y) \in \mathbb{R}^2$  is redefined as:

$$\|\nabla f(x, y)\|_2 = \sqrt{f_1^2 + f_2^2 + f_3^2 + f_4^2}, \quad (11)$$

where  $f_1, f_2, f_3, f_4$  are the transform coefficients of the image  $f(x, y)$  along directions  $\{[1, 0], [1, 1], [0, 1], [-1, 1]\}$  respectively.

#### 3.3. Non-maximum suppression

At the same time directional wavelet transforms provide more directional information, the problems caused by discrete property of image have to be solved appropriately. In the process of applying directional wavelet transforms along four directions  $\{[1, 0], [1, 1], [0, 1], [-1, 1]\}$ , the eight directions with respect to directional derivative are generated, namely  $\{[1, 0], [-1, 0]; [1, 1], [-1, -1]; [0, 1], [0, -1]; [-1, 1], [1, -1]\}$  [see Fig. 3(a), (b)]. In theory, given a pixel, two maximal directions of its derivative change should be neighboring [see Fig. 3(c)]. However, the results of the experiments show that the order of derivative directions is irregular in a number of cases. From Fig. 3(d) we see that the maximal change direction of the directional derivative is  $[1, 0]$ , but the secondary change direction is  $[-1, 1]$ . We also find that it is unsuitable to apply non-maximum suppression only along maximal change direction of the derivatives in a number of experiments. In some cases, it is still necessary to choose the secondary change direction of the derivatives. Based on the analysis mentioned above, the algorithm for non-maximum suppression is described in Table 1.

**Table 1**  
Algorithm for non-maximum suppression.

Given a pixel  $f(x, y)$ , let four vectors of its directional derivative be  $\vec{f}_1, \vec{f}_2, \vec{f}_3, \vec{f}_4$  descending sorted by their magnitude, which are generated by the transforms along the four directions.

If two directions of the vectors  $\vec{f}_1, \vec{f}_2$  are neighboring  
{ %%As demonstrated in Fig. 4(a).

- (1). Interpolate the values  $M(p_1), M(p_2)$  along the direction generated by  $\vec{f}_1, \vec{f}_2$ , where  
 $M(p_1) = (0.5|\vec{f}_2|/|\vec{f}_1|)\|\nabla f(x+1, y+1)\|_2 + (1 - 0.5|\vec{f}_2|/|\vec{f}_1|)\|\nabla f(x+1, y)\|_2$ ,  
 $M(p_2) = (0.5|\vec{f}_2|/|\vec{f}_1|)\|\nabla f(x-1, y-1)\|_2 + (1 - 0.5|\vec{f}_2|/|\vec{f}_1|)\|\nabla f(x-1, y)\|_2$ .  
 %% Notice that the gradient direction is determined by the vectors  $\vec{f}_1$  and  $\vec{f}_2$ .
- (2). If the  $f(x, y)$  is a local maximum point, that is,  
 $\|\nabla f(x, y)\|_2 > M(p_1)$  and  $\|\nabla f(x, y)\|_2 > M(p_2)$ .  
 { retain it; }

Else  
{ %%As demonstrated in Fig. 4(b).

- (1). Let  $Average = (|\vec{f}_1| + |\vec{f}_2| + |\vec{f}_3| + |\vec{f}_4|)/4$
- (2). For  $i = 1 : 2$   
 { If  $|\vec{f}_i| > Average$   
 { If the pixel  $f(x, y)$  is a local maximum point along direction of the vector  $\vec{f}_i$   
 { If  $|\vec{f}_j| < Average$ , where the vector  $\vec{f}_j$  is perpendicular to  $\vec{f}_i$ .  
 { retain it;  
 skip For loop; }  
 }  
 }  
 }%% Notice that the gradient direction is determined by the vector  $\vec{f}_1$  or  $\vec{f}_2$ .

Processing results can be seen in Fig. 5.

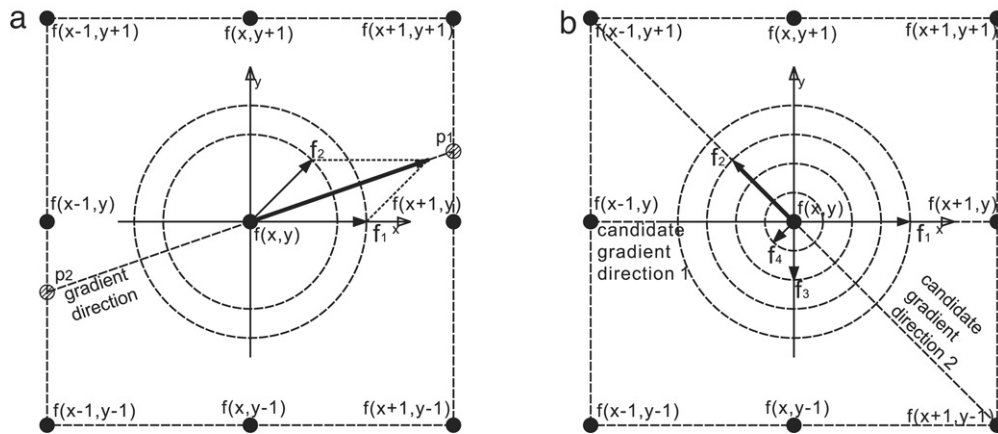


**Fig. 4.** (a) The case that two directions of the vectors  $\vec{f}_1, \vec{f}_2$  are neighboring; (b) The case that two directions of the vectors  $\vec{f}_1, \vec{f}_2$  are not neighboring.

## 4. Experimental results and conclusions

### 4.1. Experimental results

In our experiments, the processing results of each step in our approach are shown in Fig. 5. Four  $256 \times 256 \times 8$  images shown in Fig. 6 (a) (f) (k) (p) are chosen as test images. The comparisons with standard wavelet edge detection approach, Canny edge detection approach and the approach based on steerable pyramid transform [20] were used to evaluate our approach.

The results of standard wavelet edge detection approach are shown in Fig. 6 (b) (g) (l) (q), and the corresponding results of our approach are shown in Fig. 6 (e) (j) (o) (t). It is obvious that our processing results are superior to those of the standard wavelet transform. The main reason is that the standard WT involves only two directions, the horizontal and the vertical directions. The approach proposed in this paper overcomes this limitation and calculates separable wavelet transform along more directions.

The results of Canny edge detection approach are shown in Fig. 6 (c) (h) (m) (r), where we use its implementation in the image processing toolbox in Matlab to detect edges. It can be seen that their edges are slightly thinner than ours. The reason lies in applying 2D convolution kernel in Canny edge detection approach. However, edge position and orientation



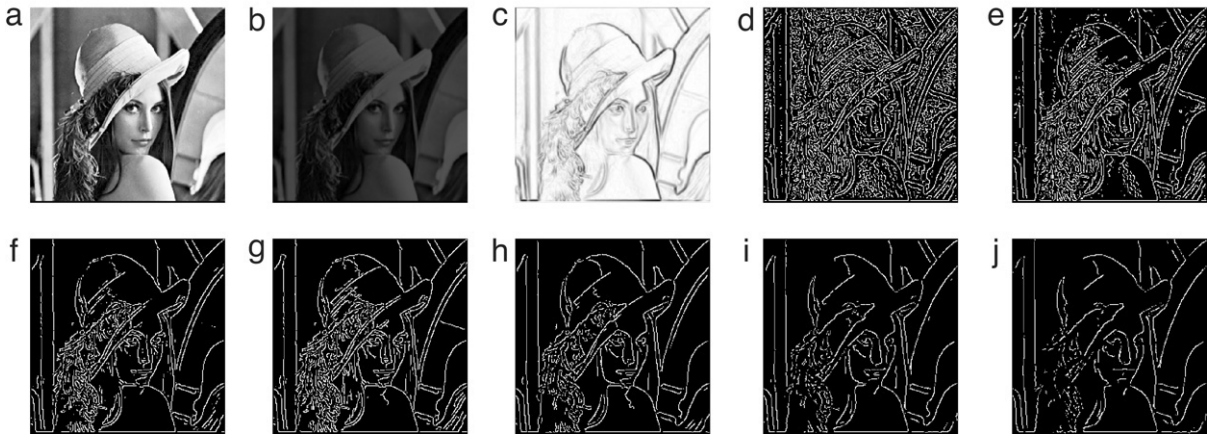


**Fig. 5.** The processing results of each step in our approach, (a) Original image; (b) Smoothed image; (c) Gradient magnitude image; (d) Local maximum image; (e) Low threshold image; (f) High threshold image; (g) The final edge image obtained in scale 1; (h) The final edge image obtained in scale 2; (i) The final edge image obtained in scale 3; (j) The final edge image obtained in scale 4.

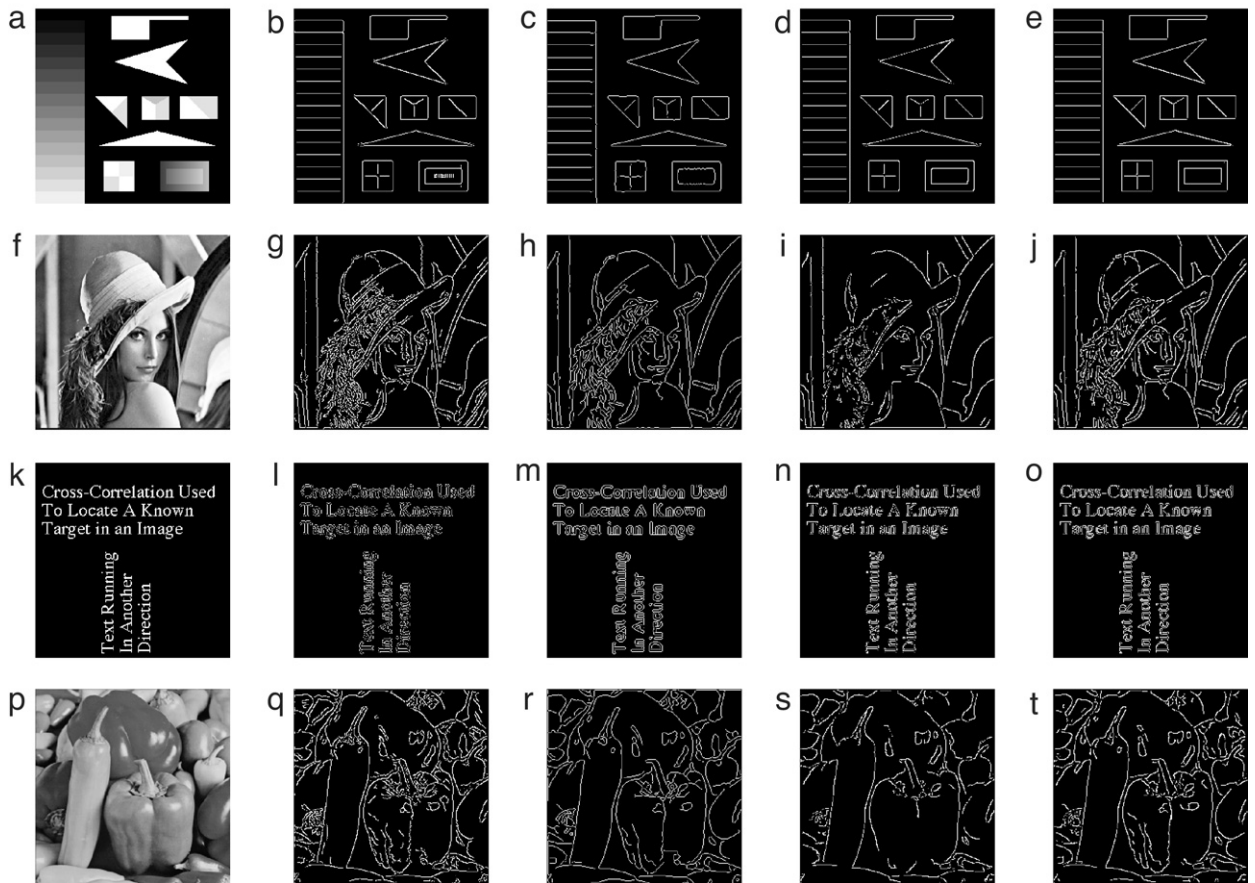


**Fig. 6.** The experimental results compared with the approach based on the standard 2D WT, the approach based on Canny detector and steerable pyramid approach proposed in [20], where (a) (f) (k) (p) are original images, (b) (g) (l) (q) are obtained by the approach based on the standard WT, (c) (h) (m) (r) are obtained by the approach based on Canny detector, (d) (i) (n) (s) are obtained by steerable pyramid approach proposed in [20], and (e) (j) (o) (t) are obtained by our methods.

in our approach are more accurate than Canny's. It can be demonstrated especially when the Fig. 6 (e) are compared with Fig. 6 (c). These benefit from more directional information that is provided by directional wavelet transform.

The results of [20] based on Steerable pyramid approach are shown in Fig. 6(d)(i)(n)(s), where the filters are “sp3Filters” with four directions. It is not difficult to see that [20] has the same merits with our approach in edge position and orientation, but the performance of ours is little superior to [20] in terms of the capacity of capturing detailed information.

#### 4.2. Computational complexity analysis and conclusion

In this subsection, we will analyze the computational complexity of our method, and compare with other popular methods in filter process. Consider an image with size  $N * N$ , and assume that sampling operations do not carry any computational cost, then we calculate the order of computational complexity of the discrete directional wavelet transform which is used in our methods, the transforms are applied along 4 directions, so  $4L$  multiplications and  $4(L - 1)$  additions are needed at each pixel, the total order of computational complexity of directional wavelet transform is  $O(4(2L - 1)N^2) = O(LN^2)$ , where  $L$  is the length of the applied filter. The computational complexity of directional wavelet transform is close to the standard WT. Because of the 2D filter structure, the computational complexity of the steerable pyramid transforms and Canny filter is slightly higher than the directional wavelet transform. Other powerful directional wavelet representations, such as ridgelets and curvelets [9,10] and iterated directional filter banks [11,12], require  $O(N^2 \log N)$  and  $O(L_1 L_2 N^2)$  operations respectively, where  $L_1$  and  $L_2$  are the sizes of non-separate 2D filters and  $L_1 L_2 \gg L$ .

Simplicity and low computational complexity of separable wavelet transforms are still maintained. The advantage of edge position and orientation accuracy is notable. Moreover, a number of experiments indicate the validity and feasibility of our approach. This new approach can be used widely in many image processing applications.

#### References

- [1] V. Torre, T.A. Poggio, On edge detection, *IEEE Trans. Pattern Anal. Mach. Intell.* 8 (2) (1986) 147–163.
- [2] T. Aydin, Y. Yemez, E. Anarim, B. Sankur, Multidirectional and multiscale edge detection via M-band wavelet transform, *IEEE Trans. Image Process.* 5 (9) (1996) 1370–1377.
- [3] L.G. Roberts, Machine perception of three-dimensional solids, in: *Optical and Electrooptical Information Processing*, MIT Press, Cambridge, MA, 1965, pp. 159–197.
- [4] I. Sobel, Neighborhood coding of binary images for fast contour following and general array binary processing, *Comput. Graph. Image Process.* 8 (1978) 127–135.
- [5] J.M.S. Prewitt, Object enhancement and extraction, in: B.S. Lipkin, A. Rosenfeld (Eds.), *Picture Analysis and Psychopictorics*, Academic Press, New York, 1970, pp. 75–149.
- [6] John Canny, A computational approach to edge detection, *IEEE Trans. Pattern Anal. Mach. Intell.* 8 (6) (1986) 679–698.
- [7] S. Mallat, S. Zhong, Characterization of signals from multiscale edges, *IEEE Trans. Pattern Anal. Mach. Intell.* 14 (7) (1992) 710–732.
- [8] S. Mallat, W.L. Hwang, Singularity detection and processing with wavelets, *IEEE Trans. Inform. Theory* 38 (2) (1992) 617–643.
- [9] E.J. Candés, D.L. Donoho, Ridgelets: A key to higher-dimensional intermittency? *Phil. Trans. R. Soc. London* 357 (1760) (1999) 2405–2509.
- [10] E.J. Candés, D.L. Donoho, Curvelets — a surprisingly effective nonadaptive representation for objects with edges, in: A. Cohen, C. Rabut, L.L. Schumaker (Eds.), *Curve and Surface Fitting*, Vanderbilt University Press, Saint-Malo, 1999, pp. 105–120.
- [11] R.H. Bamberger, M.J.T. Smith, A filter bank for the directional decomposition of images: Theory and design, *IEEE Trans. Signal Process.* 40 (4) (1992) 882–893.
- [12] M.N. Do, Directional multiresolution image representations, Ph.D. Thesis, Department of Communication Systems, Swiss Federal Institute of Technology Lausanne, November 2001.
- [13] E.P. Simoncelli, W.T. Freeman, E.H. Adelson, D.J. Heeger, Shiftable multiscale transforms, *IEEE Trans. Inform. Theory* 38 (2) (1992) 587–607.
- [14] R.A. Zuidwijk, Directional and time-scale wavelet analysis, *SIAM J. Math. Anal.* 31 (2) (2000) 416–430.
- [15] E. LePennec, S. Mallat, Image compression with geometrical wavelets, in: *IEEE Int. Conf. Image Processing*, Vancouver, Canada, September 2000, pp. 661–664.
- [16] A. Cohen, B. Matei, Compact representation of images by edge adapted multiscale transforms, in: *IEEE Int. Conf. Image Processing and Non-Linear Approximation*, Vancouver, Canada, October 2001, pp. 8–11.
- [17] V. Velisavljević, P.L. Dragotti, M. Vetterli, Directional wavelet transforms and frames, in: *Proc. IEEE Inf. Conf. Image Processing*, Rochester, NY, June 2002, pp. 589–592.
- [18] V. Velisavljević, B. Beferull-Lozano, M. Vetterli, P.L. Dragotti, Discrete multi-directional wavelet bases, in: *Proc. IEEE Int. Conf. Image Processing*, Barcelona, Spain, September 2003, pp. 1025–1028.
- [19] J.H. Conway, N.J.A. Sloane, *Sphere Packings, Lattices and Groups*, Springer, New York, NY, 1998 (Chapter 4, pp. 106–108).
- [20] Zhi-wei Kang, Jian-li Liao, Yi-gang He, Method of multi-directional image edge detection based on steerable wavelet, *J. Syst. Simul.* 18 (4) (2006) 986–988.